Applicability of Urea in the Thermodynamic Analysis of Secondary and Tertiary RNA Folding†

Valerie M. Shelton,‡ Tobin R. Sosnick,*,§ and Tao Pan*,§

Department of Chemistry and Department of Biochemistry and Molecular Biology, University of Chicago, Chicago, Illinois 60637

Received July 22, 1999; Revised Manuscript Received October 21, 1999

ABSTRACT: The equilibrium folding of a series of self-complementary RNA duplexes and the unmodified yeast $tRNA^{Phe}$ is studied as a function of urea and Mg^{2+} concentration with optical spectroscopies and chemical modification under isothermal conditions. Via application of standard methodologies from protein folding, the folding free energy and its dependence on urea concentration, the *m* value, are determined. The free energies of the RNA duplexes obtained from the urea titrations are in good agreement with those calculated from thermal melting studies [Freier, S. I., et al. (1986) *Proc. Natl. Acad. Sci. U.S.A. 83*, 9373]. The *m* value correlates with the length of the RNA duplex and is not sensitive to ionic conditions and temperature. The folding of the unmodified yeast $tRNA^{Phe}$ can be described by two Mg^{2+}-dependent transitions, the second of which corresponds to the formation of the native tertiary structure as confirmed by hydroxyl radical protection and partial nuclease digestion. Both transitions are sensitive to urea and have *m* values of 0.94 and 1.70 kcal mol^{-1} M^{-1}, respectively. Although the precise chemical basis of urea denaturation of RNA is uncertain, the *m* values for the duplexes and $tRNA^{Phe}$ are proportional to the amount of the surface area buried in the folding transition. This proportionality, 0.099 cal mol^{-1} M^{-1} $Å^{-2}$, is very similar to that observed for proteins, 0.11 cal mol^{-1} M^{-1} $Å^{-2}$ [Myers, J., Pace, N., and Scholtz, M. (1995) *Protein Sci. 4*, 2138]. These results indicate that urea titration can be used to measure both the free energy and the magnitude of an RNA folding transition.

The denaturant urea is commonly used to measure protein stability (*1*). From urea titrations, the folding free energy, ΔG, and its dependence on urea concentration, the *m* value, can be determined. The magnitude of the *m* value for proteins correlates with the increase in the solvent accessible surface area (ΔASA)[1] upon unfolding from the native state to the denatured state (*2*). For proteins, both parameters can be obtained from a single urea melting experiment. Recently, urea also has been used in RNA folding studies (*3*−*7*).

This work demonstrates the applicability of urea titration as a probe for RNA thermodynamics and presents a quantitative framework by addressing the following questions. Can urea titration of RNA duplexes reproduce the free energy values obtained from thermal melting? Can urea titration be used to obtain thermodynamic parameters for tertiary RNA folding? Can urea titration provide information about the magnitude of the structural changes in a folding transition? These questions are addressed by examining the urea and Mg^{2+} concentration dependence of two model RNA systems. The first system, representative of secondary structures, is a series of self-complementary RNA duplexes of increasing length. The second system, representative of tertiary structures, is the unmodified yeast $tRNA^{Phe}$. We find that the urea-determined values of the free energy of duplex formation are in good agreement with values calculated from the thermal denaturation studies of Turner and co-workers (*8*), and the *m* value correlates with the length of the duplex. The free energy and *m* value for $tRNA^{Phe}$ obtained from the urea (unfolding) and the Mg^{2+} (folding) titrations are identical, indicating that the tertiary folding transition of $tRNA^{Phe}$ is reversible. The *m* values for the duplexes and $tRNA^{Phe}$ are proportional to the amount of the surface area buried in each respective folding transition. Hence, urea titration is a viable method for measuring RNA stability and provides a parameter that characterizes the magnitude of the structural change in a folding transition.

MATERIALS AND METHODS

Preparation of RNA Duplexes. Self-complementary RNAs varying in length from 6 to 18 nucleotides were chemically synthesized by Dharmacon Research (Boulder, CO). The RNAs were deprotected according to the manufacturer's protocol, purified using polyacrylamide gel electrophoresis

† This work was supported by a grant from NIH (GM57880 to T.P. and T.R.S.).

* Corresponding authors. Phone: (773) 702-4179. Fax: (773) 702-0439. E-mail: taopan@midway.uchicago.edu and trsosnic@midway.uchicago.edu.

‡ Department of Chemistry.

§ Department of Biochemistry and Molecular Biology.

[1] Abbreviations: CD, circular dichroism; ΔG, free energy of the RNA structure in the absence of urea; *m*, free energy dependence on the urea concentration; *n*, Hill constant; ΔASA, differential accessible surface area.

10.1021/bi991699s CCC: $18.00
Published on Web 12/02/1999

with 7 M urea and 2 mM EDTA, and stored at −20 °C as aqueous solutions. RNA duplexes were prepared by heating in buffered solution [20 mM sodium cacodylate buffer (pH 6.6) and the appropriate sodium chloride concentration] at 90 °C for 2 min, incubating at ambient temperature for 3 min, and then incubating at the desired temperature.

Unmodified yeast $tRNA^{Phe}$ was synthesized using T7 RNA polymerase by standard in vitro transcription from a *Bst*NI-cut plasmid DNA template (*9*). The 5′ fluorescein-labeled tRNA was also synthesized by in vitro transcription as described by Fang et al. (*43*). The transcript was precipitated with ethanol, redissolved in 9 M urea and 100 mM EDTA loading buffer, purified on a polyacrylamide gel containing 7 M urea and 2 mM EDTA (to chelate residual cations), and stored in water at −20 °C.

Equilibrium Measurements. Circular dichroism (CD), absorbance, and fluorescence monitoring of Mg^{2+} and urea titrations were carried out using a Jasco J715 spectropolarimeter interfaced with a Hamilton titrator. The sample cuvette holder was outfitted with a magnetic stirrer and circulating water jacket for proper mixing and temperature control. CD data were collected at 260 nm with a 2 nm bandwidth and an acquisition time of 30 s for the RNA duplexes, but with an acquisition time of 15 s for tRNA to minimize the amount of UV cross-linking observed for this molecule (*10*). Since the equilibrium between an RNA duplex and single strands is concentration-dependent, the urea titrant contained RNA at the same concentration as in the original sample.

The $tRNA^{Phe}$ was refolded by heating in buffered solution [20 mM sodium cacodylate (pH 6.6) and varying concentrations of urea when appropriate] at 90 °C for 2 min followed by incubation at 20−25 °C for 3 min. The tRNA at this stage was designated as the U state. For urea titrations, Mg^{2+} was added and the mixture further incubated at ambient temperature for 5 min.

Folding of tRNA Monitored by Hydroxyl Radical Protection. The fraction of tRNA protected from hydroxyl radical cleavage was determined by the standard Fe(II)−EDTA footprinting method with 50 μM Fe(II) and 60 μM EDTA (*11*). The 5′ ^{32}P-labeled tRNA at 0.5 μM was heated in 20 mM sodium cacodylate (pH 6.6) with 4 M urea at 90 °C for 2 min, followed by incubation at 20−25 °C for 3 min. Varying concentrations of $MgCl_2$ were added, and the solutions were incubated at ambient temperature for an additional 5 min. Ascorbic acid and dithiotheitol were added to final concentrations of 1 and 5 mM, respectively. The hydroxyl radical generation and cleavage reactions were initiated by the addition of a 10× solution of a 1:1.2 mixture of $Fe(NH_4)_2(SO_4)_2$ and EDTA (pH 8.0). The cleavage reaction was allowed to proceed at 37 °C for 2 h and was quenched by the addition of thiourea to a final concentration of 10 mM. The reaction mixture was then separated using denaturing polyacrylamide gels containing 7 M urea, and the amount of products was quantitated using a Molecular Dynamics phosphorimager and ImageQuant software.

Folding of tRNA Monitored by Partial Nuclease Digestion. The fraction of $tRNA^{Phe}$ protected from RNase T1 cleavage, and the fraction cleaved by RNase V1, were determined by standard nuclease mapping (*12*). The RNA was renatured by heating in 20 mM sodium cacodylate (pH 6.6) with 4 M urea at 90 °C for 2 min, followed by incubation at ambient temperature for 3 min. Varying concentrations of $MgCl_2$ were added, and the solutions were incubated at ambient temperature for an additional 5 min. The final $tRNA^{Phe}$ concentration was 0.5 μM, containing a trace amount of 5′ ^{32}P-labeled $tRNA^{Phe}$. The nuclease reactions were initiated by adding 0.05 unit/μL RNase T1 or 0.1 milliunit/μL RNase V1 and allowed to proceed for 5 min at 37 °C. The cleavage reactions were quenched by rapidly cooling on ice and adding an equal volume of gel loading buffer containing 9 M urea/50 mM EDTA (pH 8.0) and 0.5 μg of unlabeled *Escherichia coli* tRNA.

Calculation of the Accessible Surface Area (ΔASA). The accessible surface area buried upon duplex formation was estimated from the crystal structures of RNA duplexes using the maximal exposed surfaces of adenosine (503 Å^2), cytosine (485 Å^2), guanosine (526 Å^2), and uridine (435 Å^2) (Table 3 in ref *13*). Using the accessible surface area calculation of the helical regions in yeast $tRNA^{Phe}$, the average ΔASAs for an A-U and a C-G base pair were calculated to be 602 and 654 Å^2, respectively (Table 6 in ref *13*). A value of 531 Å^2 was used for the more exposed, terminal G-C base pair. The ΔASA for the yeast $tRNA^{Phe}$ is 23 674 Å^2, as calculated by Alden and Kim (*13*).

Data Analysis. The stability of the RNA duplexes defined by

$$\Delta G = -RT \ln K_{eq} = -RT \ln \frac{[\text{duplex}]}{[\text{monomer}]^2} \qquad (1)$$

where R is the gas constant and T is the absolute temperature, was calculated assuming a linear free energy dependence on the urea concentration

$$\Delta G(\text{urea}) = \Delta G + m[\text{urea}] \qquad (2)$$

where ΔG is the free energy at 0 M urea and m is the dependence of ΔG on urea concentration (units of kilocalories per mole per molar urea). The urea-dependent CD signal was fit to the sum of the signals from the duplex and the single-strand fractions obtained by combining eqs 1 and 2 (*14*):

$$\Delta\epsilon_{obs} = \Delta\epsilon_{init} - \frac{\Delta\epsilon_{init} - \Delta\epsilon_{final}}{4[S]_T} \times [-1 + \sqrt{1 + 8[S]_T/e^{-(\Delta G - m[\text{urea}])/RT}}]e^{-(\Delta G - m[\text{urea}])/RT} \qquad (3)$$

where $[S]_T$ is the total strand concentration, $\Delta\epsilon_{obs}$ is the observed signal intensity, and $\Delta\epsilon_{init}$ and $\Delta\epsilon_{final}$ are the spectroscopic signals for the duplex and single-strand forms, respectively. The sloping CD baselines for the 100% duplex and 100% single-strand forms of the RNA were determined by altering the NaCl concentration or temperature such that the desired state was stable over a large range of urea concentrations (data not shown).

The yeast $tRNA^{Phe}$ undergoes two Mg^{2+}-dependent structural transitions

$$U \xleftrightarrow{K_{Mg1},n_1} I \xleftrightarrow{K_{Mg2},n_2} N$$

where K_{Mg1} and K_{Mg2} are the Mg^{2+} midpoints and n_1 and n_2 are the Hill constants of the U-to-I and I-to-N transitions, respectively. These transitions may be described with a

Table 1: Urea Melting of Self-Complementary RNA Duplexes

RNA duplex sequence	[NaCl] (M)	temp (°C)	m (kcal mol^{-1} M^{-1})	ΔG (kcal mol^{-1})[a]	ΔG_{calc} (kcal mol^{-1})[b]
GCA GUA GUC GAC UAC UGC	0.5	70	1.17 ± 0.02	14.3 ± 0.1	(15.3)
	1.0	70	1.36 ± 0.03	16.3 ± 0.2	**15.3**
GCA GUA GCU ACU GC	0.5	60	1.06 ± 0.02	15.3 ± 0.1	(19.0)
	0.5	70	1.05 ± 0.04	10.8 ± 0.1	(16.5)
GCA GUA CUG C	0.25	50	0.84 ± 0.02	11.0 ± 0.1	(13.4)
	0.5	50	0.83 ± 0.01	12.1 ± 0.1	
	0.75	50	0.78 ± 0.03	12.2 ± 0.1	
GUA AUA UUA C	0.5	20	0.74 ± 0.04	11.0 ± 0.2	(10.6)
	1.0	25	0.86 ± 0.06	10.0 ± 0.2	**9.6**
GCA UGC	0.5	20	0.64 ± 0.10	10.8 ± 0.4	(10.2)
	1.0	20	0.72 ± 0.06	12.1 ± 0.2	**10.2**

[a] Referenced to 1 M standard state. [b] Calculated for 1 M NaCl from $\Delta G = \Delta H - T\Delta S$ using ΔH and ΔS values from ref *8*. Values in bold can be directly compared to those obtained from urea melting at 1 M NaCl.

cooperative Mg^{2+} binding model (*43*)

$$\frac{[I]}{[U]+[I]} = \frac{[Mg^{2+}]^{n_1}}{[Mg^{2+}]^{n_1} + (K_{Mg1})^{n_1}} \quad (4a)$$

$$\frac{[N]}{[I]+[N]} = \frac{[Mg^{2+}]^{n_2}}{[Mg^{2+}]^{n_2} + (K_{Mg2})^{n_2}} \quad (4b)$$

The CD data were fit as a linked equilibrium between these two transitions according to

$$\Delta\epsilon_{obs} = f_U\Delta\epsilon_U + f_I\Delta\epsilon_I + f_N\Delta\epsilon_N = \frac{\Delta\epsilon_U + \Delta\epsilon_I\left(\frac{[Mg^{2+}]}{K_{Mg1}}\right)^{n_1} + \Delta\epsilon_N\left(\frac{[Mg^{2+}]}{K_{Mg1}}\right)^{n_1}\left(\frac{[Mg^{2+}]}{K_{Mg2}}\right)^{n_2}}{1 + \left(\frac{[Mg^{2+}]}{K_{Mg1}}\right)^{n_1} + \left(\frac{[Mg^{2+}]}{K_{Mg1}}\right)^{n_1}\left(\frac{[Mg^{2+}]}{K_{Mg2}}\right)^{n_2}} \quad (5a)$$

$$f_U + f_I + f_N = 1 \quad (5b)$$

where $\Delta\epsilon_{obs}$ is the observed signal intensity and $\Delta\epsilon_U/f_U$, $\Delta\epsilon_I/f_I$, and $\Delta\epsilon_N/f_N$ are the spectroscopic signal/fraction ratios of the U, I, and N states, respectively. The hydroxyl radical protection data were fit only to the I-to-N transition using eq 4b, since the protection does not change for the U-to-I transition for this tertiary RNA. The urea titration data of the yeast $tRNA^{Phe}$ were fit according to

$$\Delta\epsilon_{obs} = \frac{\Delta\epsilon_I + \Delta\epsilon_N e^{[-(\Delta G_2 + m_2[urea])/RT]}}{1 + e^{[-(\Delta G_2 + m_2[urea])/RT]}} \quad (6)$$

assuming a linear dependence on the urea concentration for the stability of the I-to-N (ΔG_2 and m_2) transitions. From the free energies extrapolated to zero denaturant obtained from urea titrations conducted at two different Mg^{2+} concentrations, the Hill constant for the I-to-N transition was calculated according to

$$n_2 = \frac{\Delta G_2{}^i - \Delta G_2{}^j}{RT\ln\left(\frac{[Mg^{2+}]_j}{[Mg^{2+}]_i}\right)} \quad (7)$$

where $\Delta G_2{}^i$ and $\Delta G_2{}^j$ are the stabilities obtained from the urea titration conducted at $[Mg^{2+}]_i$ and $[Mg^{2+}]_j$, respectively (*43*).

Data analysis was performed using the Microcal Origin version 5.0 nonlinear fitting routine. Unless otherwise noted, errors listed are the standard deviation calculated by the fitting algorithm and reflect the statistical uncertainty of the fitted parameters.

RESULTS

Sequence Design of RNA Duplexes. Self-complementary RNAs 6, 10, 14, and 18 nucleotides long were chosen to cover a broad size range of duplexes that still could be completely denatured by urea at moderate temperatures. The self-complementarity circumvented the complication of having to determine separate values for the concentration of each strand. The sequences were designed to minimize the extent of possible hairpin formation. Four of the five duplexes have G-C to A-U ratios of 60/40 (Table 1). The fifth, a 10-nucleotide duplex containing 80% A/U, was used to examine the sequence dependence of the *m* values. All sequences were designed to have G-C closing pairs in the duplex to minimize fraying.

Urea Unfolding of RNA Duplexes. Both UV absorbance and CD can be used to monitor changes in RNA structure (*15*, *16*). The maxima in the near-UV CD spectra are at ~270 and ~260 nm for the single-stranded and duplex forms, respectively (Figure 1). The decrease in the level of base stacking upon duplex melting results in an increase in the absorbance and a decrease in the CD in the vicinity of 260 nm. Urea also absorbs at these wavelengths so that absorbance-monitored titrations have sharply sloping baselines (data not shown). Hence, CD is used exclusively in this work for the urea melting studies.

The free energy of duplex formation, ΔG, and the sensitivity to urea concentration, the *m* value, are obtained from urea titrations (Table 1). As expected, duplex stability increases with increasing monovalent cation concentration and decreasing temperature. At 1 M NaCl, the ΔG obtained from urea melting is within 5−20% of the value calculated from parameters obtained from thermal melting studies conducted by Turner and co-workers (*8*). The agreement between the ΔG values from chemical and thermal denaturation indicates that both methods report on the same unfolding transition.

The *m* values for the duplexes increase proportionally with their length (Table 1). The correlation is the same for the duplexes with 40 and 80% A/U content. A similar correlation between size and *m* values is observed for globular proteins

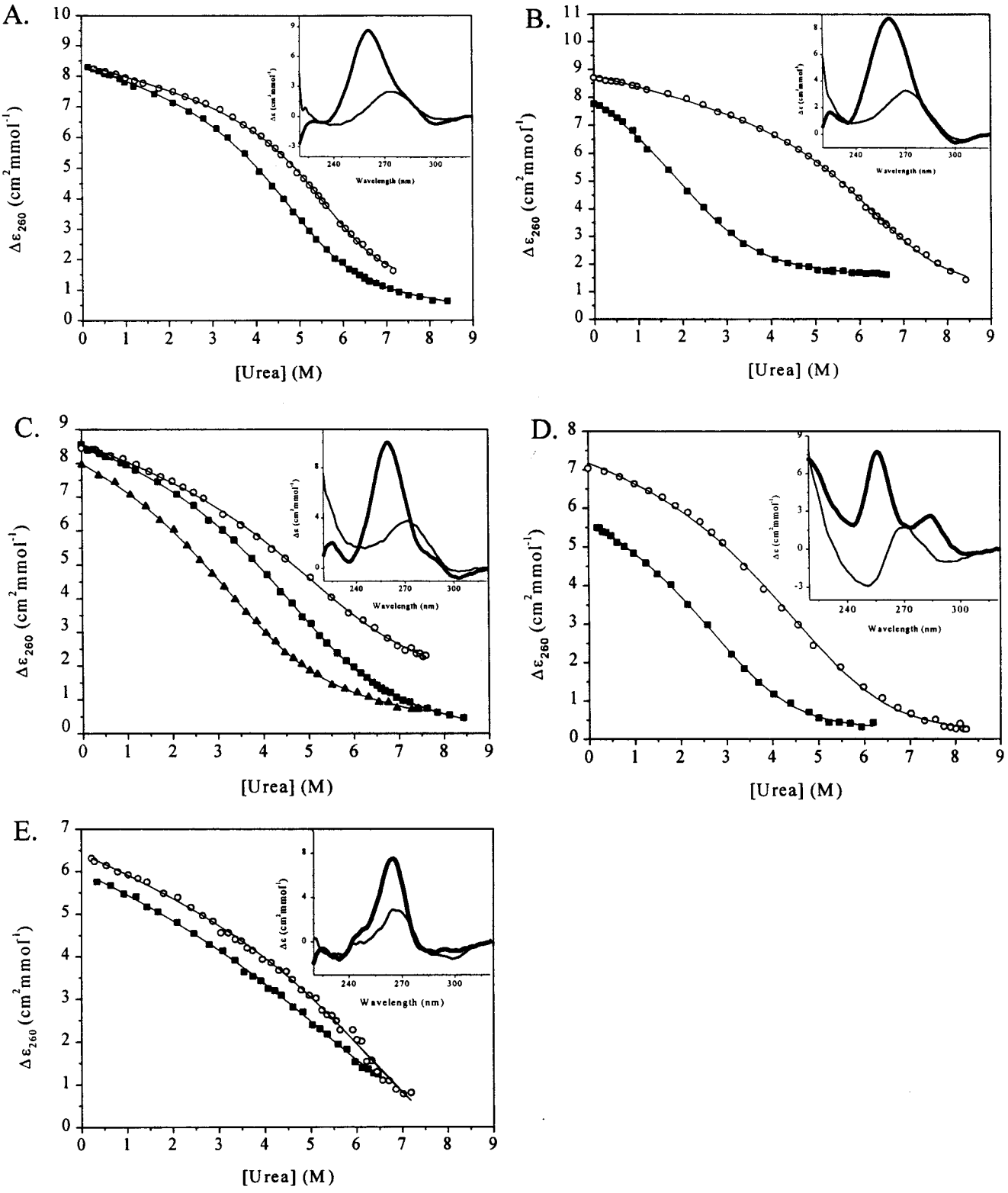

FIGURE 1: Urea titration of self-complementary RNA duplexes in 20 mM sodium cacodylate (pH 6.6). The insets in panels A−D show relevant CD spectra in (thick line) 0 M urea and (thin line) 8.4 M urea (unless otherwise noted): (A) 2 μM 18mer at 70 °C with (■) 0.5 M NaCl and (○) 1 M NaCl, (B) 2 μM 14mer with 0.5 M NaCl at (○) 60 and (■) 70 °C, (C) 2 μM 10mer (40% A/U) at 50 °C with (▲) 0.25 M NaCl, (■) 0.5 M NaCl, and (○) 0.75 M NaCl, (D) 2 μM 10mer (80% A/U) with (○) 0.5 M NaCl at 20 °C and (■) 1 M NaCl at 25 °C, and (E) 2 μM 6mer at 20 °C with 0.5 M NaCl (■) and 3 μM 6mer with 1 M NaCl (○). The inset in panel E shows the CD spectrum at 260 nm in (thick line) 0 M urea and (thin line) 7.2 M urea.

ranging from 50 to 400 amino acids (*2*). For proteins, the *m* value is well correlated with the difference in solvent accessible surface area (ΔASA) between the unfolded and the native state. Since the amount of surface burial in RNA duplexes also increases with size, the proportional increase of the *m* value suggests a similar correlation for RNA folding. The increase in surface area upon duplex denaturation represents the increased level of solvent exposure of nucle-

otide bases and ribose moieties. These results demonstrate that urea titration can be used to measure the stability of RNA secondary structures.

Folding and Unfolding of Unmodified Yeast tRNA^{Phe}. A major consideration in tertiary RNA folding is that multiple structural transitions can exist. Since the secondary structure of an RNA can be independently stable, an intermediate I state may be populated prior to the formation of the tertiary structure. Therefore, unlike the secondary structure studies, the formation of the tertiary structure may include at least two structural events, a U-to-I transition and an I-to-N transition. An additional consideration is that RNA tertiary structures often require the specific binding of divalent metal ions such as Mg^{2+}. We have applied a cooperative Mg^{2+} binding model to describe the Mg^{2+} concentration dependence of these transitions

$$A + nMg^{2+} \xrightarrow{K_{Mg}} [A\cdot(Mg^{2+})_n]$$

In this model, two parameters are required to describe a transition, the Mg^{2+} midpoint, K_{Mg}, and the degree of cooperativity defined in terms of a Hill constant, n. In this model, the Mg^{2+}-dependent free energy of each structural transition is given by $\Delta G = -nRT \ln([Mg^{2+}]/K_{Mg})$ (*43*).

We choose to use unmodified yeast tRNA^{Phe} to demonstrate the feasibility of urea titration in studying thermodynamics of tertiary RNA folding. The native structure of this tRNA consists of two coaxially stacked helices that are approximately perpendicular to each other (*17*, *18*). This L-shaped conformation is stabilized by tertiary structure in the elbow region. Previous studies of tRNA thermodynamics roughly fall into two categories. Early studies in the 1970s often dealt with the unfolding sequence of modified tRNAs in thermal melting as monitored by UV absorbance or NMR (*19*−*22*). More recent studies dealt with the formation of the tertiary structure of the unmodified tRNA transcripts using chemical and nuclease mapping, aminoacylation, UV absorbance, NMR, and other biophysical methods that correlate with the overall shape of the tRNA (*23*−*28*). The general conclusion from the recent studies is that the unmodified tRNA^{Phe} can adopt the same tertiary structure as the modified tRNA^{Phe} found in the cell.

In this work, we first use chemical mapping methods to probe the formation of the tertiary tRNA structure as a function of Mg^{2+} concentration in the presence of urea. We then apply spectroscopic methods without affecting the chemical integrity of this tRNA to assess both transitions as a function of Mg^{2+} and urea concentration.

Tertiary Folding of tRNA Monitored by Hydroxyl Radical Protection and Partial Nuclease Digestion. Hydroxyl radical protection is commonly used to monitor the formation of Mg^{2+}-dependent tertiary RNA structures (*11*, *29*, *30*). The Fe(II)−EDTA complex interacts with a dioxygen species to generate hydroxyl radicals. The hydroxyl radical attacks the ribose moiety along the surface of RNA. Secondary reactions of the ribose-centered radicals result in cleavage of the ribose−phosphate backbone (*31*, *32*). Because of the small size of the hydroxyl radical, only the ribose moieties of residues buried within the tertiary RNA structure are protected from cleavage. The hydroxyl radical protection has been successfully applied to determine the folding of the

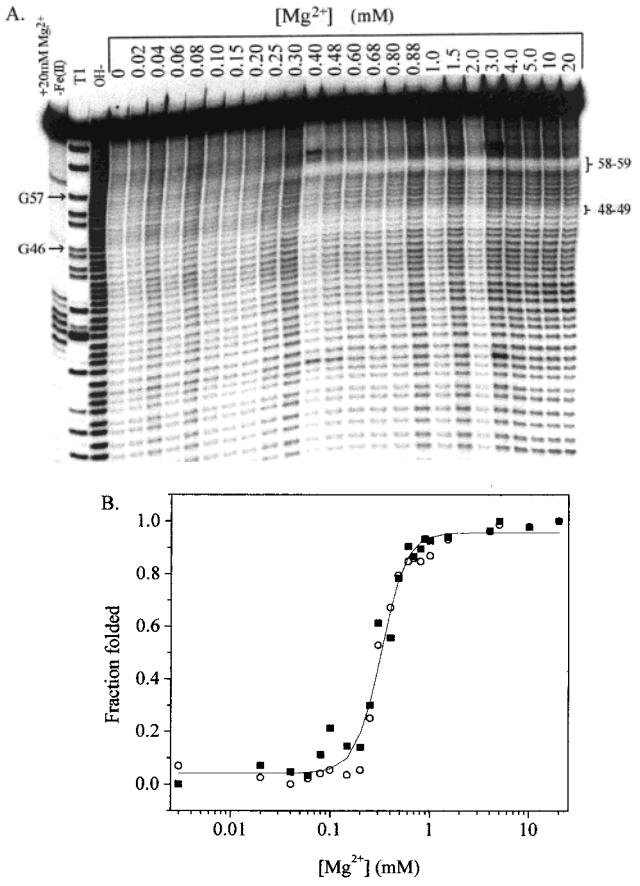

FIGURE 2: Hydroxyl radical cleavage protection of unmodified yeast tRNA^{Phe} in 4 M urea and 20 mM sodium cacodylate at pH 6.6 and 37 °C. (A) Mg^{2+} concentration dependence. The protected regions include nucleotides 58, 59, 48, and 49: (T1) partial T1 ribonuclease digestion under denaturing conditions and (OH-) partial alkaline hydrolysis of the same RNA. (B) Quantitation of hydroxyl radical protection at (■) nucleotides 48 and 49 and (○) nucleotides 58 and 59. The plot of the fraction folded vs Mg^{2+} concentration is fit with eq 4b to obtain K_{Mg} and n.

unmodified yeast tRNA^{Phe} with or without Mg^{2+} (*11*). Regions in tRNA^{Phe} significantly protected against hydroxyl radical attack include nucleotides 48, 49, and 58−60; these nucleotides are the least exposed in the crystal structure.

We determined the protection of nucleotides 48, 49, 58, and 59 in the unmodified yeast tRNA^{Phe} as a function of Mg^{2+} concentration in the presence of 4 M urea at 37 °C (Figure 2A). The protection pattern in the tRNA^{Phe} structure in 4 M urea at high Mg^{2+} concentrations is very similar to those observed in the absence of urea (data not shown). The cleavage protection can be quantitated as the fraction folded when normalized to the cleavage with none (no Mg^{2+}) and all (10 mM Mg^{2+}) of the molecules folded. The plot of the fraction folded versus Mg^{2+} concentration can be fit with a binding model (eq 4b) to obtain a K_{Mg} of 0.32 ± 0.01 mM and a Hill constant of 3.5 ± 0.4 (Figure 2B). The similarity in the protection pattern and the large Hill constant strongly suggests that in the presence of sufficiently high Mg^{2+} concentrations, tRNA^{Phe} can form its native structure even in the presence of 4 M urea.

Partial nuclease digestion using nucleases V1 and T1 is used to detect structural transitions in 4 M urea involving specific nucleotide bases (Figure 3A). The nuclease V1 cuts double-stranded or stacked regions in RNA, whereas the

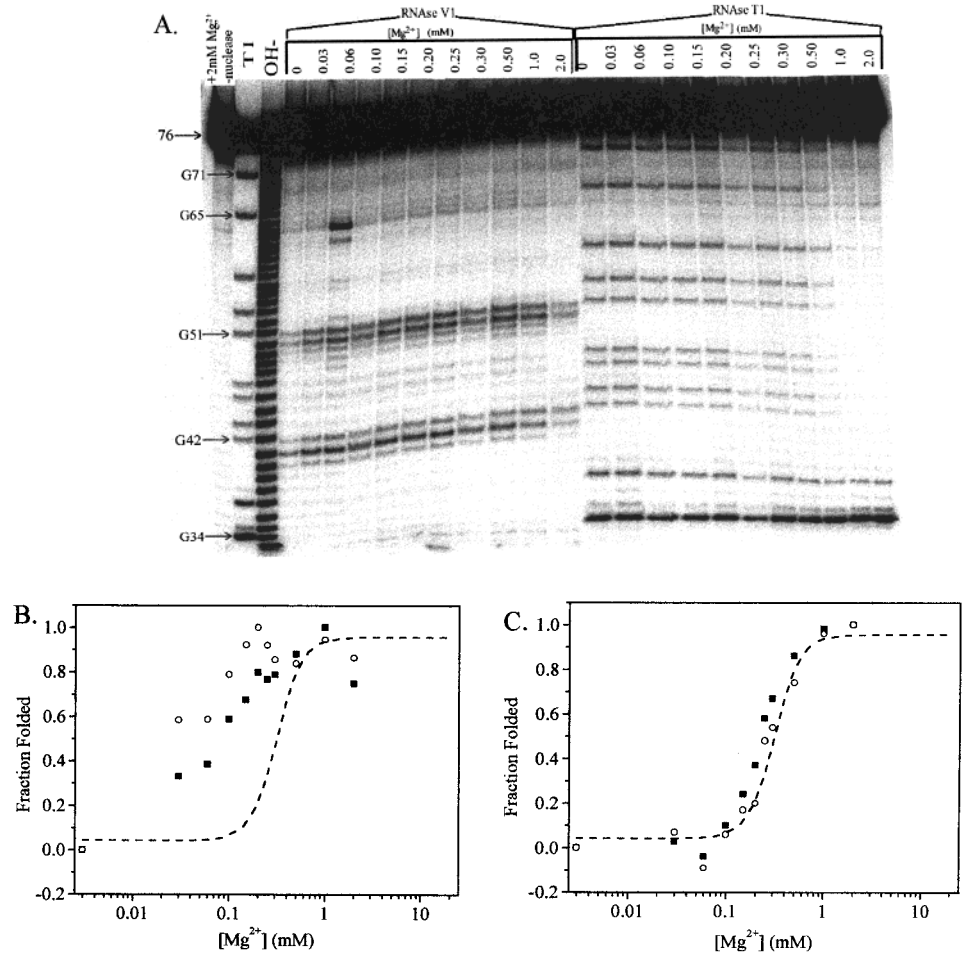

FIGURE 3: (A) Partial V1 and T1 ribonuclease digestion of 0.5 μM tRNA^{Phe} in 4 M urea and 20 mM sodium cacodylate at pH 6.6 and 37 °C as a function of Mg^{2+} concentration: (T1) partial T1 ribonuclease digestion under denaturing conditions and (OH-) partial alkaline hydrolysis of the same RNA. (B) Fraction folded as a function of Mg^{2+} concentration monitored by V1 cleavage at (■) nucleotides 50 and 51 and (○) nucleotides 41 and 42. The amount of V1 cuts at nucleotide 37 was used for normalization. (- - -) Data fit of hydroxyl radical cleavage protection from Figure 2B. (C) Fraction folded as a function of Mg^{2+} concentration monitored by protection from T1 cleavage at (■) nucleotide 46 and (○) nucleotide 57. The amount of T1 cuts at nucleotide 34 was used to normalize raw data for T1 mapping. (- - -) Data fit of hydroxyl radical cleavage protection.

nuclease T1 cuts the exposed G residues in the single-stranded regions. The amount of V1 and T1 nuclease cuts is strongly dependent on Mg^{2+} concentration, but in significantly different ways. The amount of V1 cuts increases with Mg^{2+} concentration in the range of 0−0.2 mM, but remains unchanged from 0.2 to 2 mM Mg^{2+}. The amount of T1 cuts remains unchanged in the range of 0−0.1 mM Mg^{2+}, but decreases sharply from 0.1 to 2 mM Mg^{2+} (Figure 3B,C). The dependence of the amount of T1 cuts on Mg^{2+} concentration is the same as observed for the hydroxyl radical protection (Figure 3B). Hence, nuclease V1 (helix formation) reports on the U-to-I transition, while nuclease T1 (single-strand cleavage) reports on the I-to-N transition.

Tertiary Folding of tRNA Monitored by CD. Both transitions can be monitored by CD at 260 nm ($\Delta\epsilon_{260}$) in urea (Figure 4A). The values of $\Delta\epsilon_{260}$ for the N state at high, saturating Mg^{2+} concentrations are very similar at all urea concentrations that were studied. This insensitivity suggests that the structure of the N state is insensitive to urea, in agreement with the hydroxyl radical measurements. The magnitude of the CD change of the I-to-N transition is rather insensitive to urea (Figure 4A), suggesting that the structure of the I state also is reasonably insensitive to urea. The Mg^{2+}-free U state, however, is sensitive to urea as indicated by a decrease in $\Delta\epsilon_{260}$. This result is consistent with urea disrupting the residual structure in the U state. However, essentially no further change in $\Delta\epsilon_{260}$ is observed beyond 4 M, indicating that all the residual structure has melted at >4 M urea and 37 °C in the absence of Mg^{2+}.

Urea increases the Mg^{2+} requirement for both folding transitions. Since the transitions are not fully separated, they are fit simultaneously with a linked equilibrium formula (eq 5) to obtain the K_{Mg} and n for each transition (Table 2). These values for the I-to-N transition in 4 M urea are the same as those obtained from hydroxyl radical protection and T1 nuclease mapping. The values for the first transition (U-to-I) are in good agreement with those obtained from V1 nuclease mapping. These identities indicate that CD reports on the same structural transitions as those observed in standard chemical and nuclease mapping techniques, and provides additional support for the three-state folding model.

The m values for the U-to-I and I-to-N transitions can be obtained from the increase in the midpoints of Mg^{2+} titrations, K_{Mg}(urea), conducted at various urea concentrations. Specifically, the m value is the slope of the plot of the folding free energy at 1 M Mg^{2+} standard state, defined as $\Delta G = -nRT \ln[K_{Mg}(\text{urea})]$, versus urea concentration (Figure 4B). Just as for the duplexes, the free energy for both folding

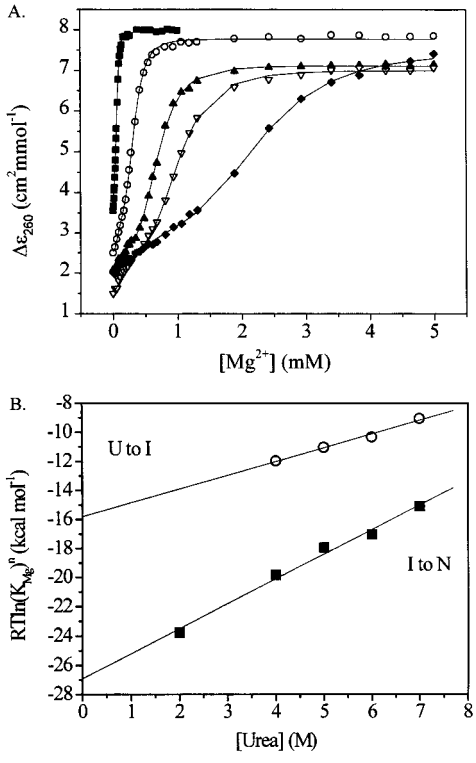

FIGURE 4: (A) Mg^{2+} titration of 0.5 μM $tRNA^{Phe}$ in 20 mM sodium cacodylate at pH 6.6 and 37 °C, monitored by CD at 260 nm in (■) 2, (○) 4, (▲) 5, (▽) 6, and (◆) 7 M urea. The data are fit with eq 5 as two linked equilibria. (B) Determination of the *m* values (slope) from Mg^{2+} titration data for (■) the I-to-N transition ($m = 1.70 \pm 0.10$ kcal mol^{-1} M^{-1}, $r^2 = 0.989$) and (○) the U-to-I transition ($m = 0.94 \pm 0.08$ kcal mol^{-1} M^{-1}, $r^2 = 0.986$).

Table 2: Mg^{2+} Titration of the Unmodified Yeast $tRNA^{Phe}$ at Constant Urea Concentrations

[urea] (M)	K_{Mg1} (mM)	n_1	K_{Mg2} (mM)	n_2
2			0.065 ± 0.008	3.1 ± 0.5
4	0.061 ± 0.036	1.9 ± 1.1	0.32 ± 0.005	3.4 ± 0.1
5	0.13 ± 0.04	1.9 ± 0.8	0.69 ± 0.01	4.1 ± 0.1
6	0.23 ± 0.09	1.4 ± 0.3	1.0 ± 0.01	3.8 ± 0.1
7	0.65 ± 0.21	1.6 ± 0.3	2.2 ± 0.03	4.1 ± 0.2

transitions of $tRNA^{Phe}$ has a linear relationship with urea concentration. The *m* values for the U-to-I and I-to-N transitions are 0.94 ± 0.08 and 1.70 ± 0.10 kcal mol^{-1} M^{-1}, respectively. A constant *m* value for the U-to-I transition is expected only at >4 M urea because the amount of structure in the starting, U state remains constant and a constant amount of area is buried in the transition.

The CD measurements were conducted using a version of $tRNA^{Phe}$ having a fluorescein covalently attached to the 5′ end. To confirm that the incorporation of the chromophore had a minimal effect on folding, Mg^{2+} titrations were conducted with an unmodified $tRNA^{Phe}$ containing a 5′-triphosphate at 4 and 6 M urea. The CD signal can be fit with two transitions with K_{Mg} and *n* values similar to those of the fluorescein-containing version (data not shown), indicating that the chromophore does not have a significant effect on the folding of this tRNA.

Urea Titration of $tRNA^{Phe}$. An alternative method for determining ΔG, *n*, and *m* is to conduct urea titration at a fixed Mg^{2+} concentration (Figure 5). As expected, the urea concentration required to unfold $tRNA^{Phe}$ increases with

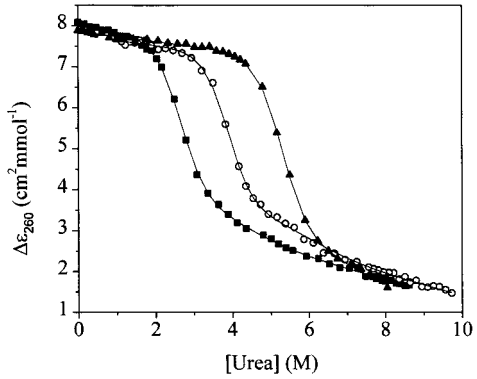

FIGURE 5: Urea titration of 0.5 μM $tRNA^{Phe}$ in 20 mM sodium cacodylate at pH 6.6 and 37 °C monitored by CD at 260 nm with (■) 0.1, (○) 0.3, and (▲) 0.5 mM Mg^{2+}. The data are fit to a single N-to-I unfolding transition according to eq 6.

increasing Mg^{2+} concentrations. However, the *m* value is independent of Mg^{2+} concentration. Starting from the N state (>0.1 mM Mg^{2+}), a single urea-induced unfolding transition is observed (Table 3). This corresponds to the N-to-I transition, the reverse process of the I-to-N transition observed in Mg^{2+} (folding) titrations for the following reasons. (i) The *m* value obtained from urea melting is identical to the value obtained from Mg^{2+} titrations. (ii) The ΔG values determined from the urea titrations are the same as those calculated from the Mg^{2+} titrations. (iii) The ΔG values obtained from urea titrations at different Mg^{2+} concentrations can be used to calculate the Hill constant of this transition (eq 7). The Hill constant obtained in this fashion is in excellent agreement with that obtained from the Mg^{2+} titrations. Hence, urea titrations provide a viable method for measuring the stability of tertiary RNAs.

DISCUSSION

Application of Urea to Studying Secondary and Tertiary RNA Stability. We have shown here that the nonionic denaturant urea can be used to measure the stability of RNA secondary and tertiary structures. The folding free energy increases linearly with the urea concentration, as also seen in protein folding. This linear dependence, defined in terms of the *m* value, directly relates to the amount of structural change in the folding transition.

The stability measured using urea titration of the RNA duplexes quantitatively reproduces values determined from parameters obtained from thermal melting studies (*8*). The Mg^{2+}-dependent formation of tertiary $tRNA^{Phe}$ structure involves two structural transitions. These transitions are described with two additional parameters related to the Mg^{2+} concentration dependence, the midpoint, K_{Mg}, and the Hill constant, *n*. The addition of urea shifts both transitions to higher Mg^{2+} concentrations, but does not change the Hill constant. Additionally, the magnitude of the near-UV CD signal change for the I-to-N transition does not change in the presence of urea, indicating that the denaturant does not measurably alter the structure of the I and N states (given the presence of the appropriate concentrations of Mg^{2+} for forming each state). Furthermore, the values for ΔG, *n*, and *m* determined from the urea titrations are the same as those determined from the Mg^{2+} titrations. These results indicate that urea melting can be used reliably to obtain thermody-

Table 3: Urea Melting of the Unmodified Yeast tRNA^{Phe} at Constant Mg^{2+} Concentrations

[Mg^{2+}] (mM)	ΔG_2^a (kcal mol^{-1})	m_2^a (kcal mol^{-1} M^{-1})	n_2^b	ΔG_2^c (kcal mol^{-1})	m_2^c (kcal mol^{-1} M^{-1})	n_2^c
0.1	-4.4 ± 0.2	1.64 ± 0.06	4.1 ± 0.1	-4.2 ± 0.5	1.70 ± 0.10	3.7 ± 0.2
0.3	-7.1 ± 0.2	1.71 ± 0.05		-6.9 ± 0.5		
0.5	-8.5 ± 0.3	1.62 ± 0.05		-8.2 ± 0.5		

[a] From eq 6. [b] From eq 7. [c] Calculated from data obtained from Mg^{2+} titrations (Table 2 and Figure 4). From eq 3 in Fang et al. (*43*).

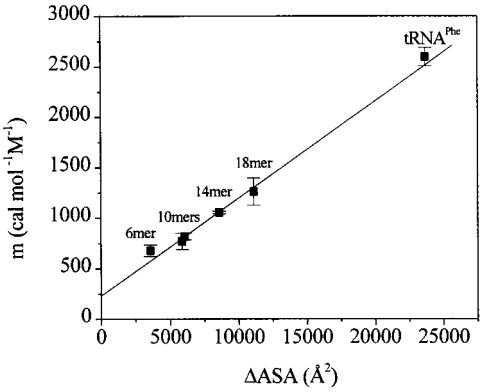

FIGURE 6: Correlation between the *m* value and ΔASA. Each point represents an average value of separate determinations. The error bars are the standard deviations of the mean values. Slope = 0.099 ± 0.004 cal mol^{-1} M^{-1} Å^{-2}; *y*-intercept = 228 ± 47 cal mol^{-1} M^{-1}, and $r^2 = 0.994$.

namic parameters for the folding of RNA tertiary structures as well as secondary structures.

Interpretation of the m Value. Whereas thermal melting measurements can provide information about the Δ*H* and Δ*S* of a folding transition, urea titrations yield a complementary parameter, the *m* value, which is the change in Δ*G* per added mole of urea per liter. This parameter provides information about the extent of structural change in the transition. For protein stability studies, *m* values correlate with the change in the solvent accessible surface area upon unfolding (*2*). The *m* values observed in this study for the RNA duplexes and tRNA^{Phe} also are linearly correlated with the calculated ΔASA (Figure 6). The change in the accessible surface area upon duplex formation is calculated from the difference of the accessibility of nucleotide bases and ribose moieties in the extended single-stranded form and in the duplex form. The ΔASA for RNA duplexes is calculated from crystal structures of RNA based on the criteria outlined in ref *13*. The *m* value for the tRNA^{Phe} in this plot represents the sum of the *m* values of the U-to-I and I-to-N transitions.

As with protein folding (*33*, *34*), whether the unfolded or denatured state of the duplexes and tRNA^{Phe} is well-described by a fully extended strand is not known (*35*). Hence, the ΔASA calculations are subject to some error. However, the denaturation experiments are conducted in the presence of urea that also disrupts residual structure. We observe a constant *m* value over an extended range of urea concentrations that argues for an insignificant amount of urea sensitive surface area buried in the denatured state.

The slope of the plot of *m* versus ΔASA (0.099 ± 0.004 cal mol^{-1} M^{-1} Å^{-2}) is surprisingly similar to the slope observed for proteins (0.11 cal mol^{-1} M^{-1} Å^{-2}) (*2*). Presumably, this similarity reflects a common mechanism of urea denaturation for these two biopolymers. At least three mechanisms, one direct and two indirect, can be postulated for urea denaturation. Urea can directly interact with the polymer, and unfolding occurs due to an increased level of interaction with the more exposed state (*36*). Alternatively, urea may operate indirectly by altering the solvent's hydrogen bonding network which can lead to increased solubility of chemical entities, particularly hydrophobic groups (*15*), although urea is also known to solubilize hydrophilic groups (*36*, *37*). The direct mechanism is supported by recent calculations which indicate that urea only minimally perturbs the hydrogen bonding geometry of water (*38*). In both mechanisms, the chemical nature of the biopolymer is relevant. A third mechanism which does not depend on the chemical character of the biopolymer is due to a change in water's surface tension. This change alters the free energy of forming the larger cavity required to encompass the more extended, unfolded chain. However, as pointed out by Breslow and Guo (*39*), the surface tension of water increases with urea concentration which would argue for an increase, rather than the observed decrease, in stability. Hence, either of the first two mechanisms is more applicable, and the chemical nature of the biopolymer probably is relevant to the correlation between ΔASA and *m* values.

The above arguments suggest a commonality between protein and RNA with regard to the chemical character of moieties that become buried upon folding. In fact, the major chemical constituents buried in RNA and protein folding are qualitatively similar: hydrogen bond donors and acceptors along with aromatic and hydrophobic groups. The major difference is the phosphodiester backbone of the RNA which is largely exposed in both the folded and unfolded states, and a change in its solubility may not greatly affect the overall folding equilibrium of RNAs. The folding of the A-form RNA helix results in the burial of about 63% of the maximal solvent accessible surface with polar groups comprising ~45% of the buried surface (*13*). The folding of globular proteins buries about ~70% of the maximal surface with polar side chains comprising ~30% of the buried surface (*40*). The yeast tRNA^{Phe} buries ~64% of its maximal surface, with the bases being slightly more exposed and phosphate oxygens being less exposed than in A-form helices. Recently, Bolen and co-workers determined that the solubilities per square angstrom for the protein backbone and side chains, both hydrophobic and hydrophilic, are nearly equivalent (*37*). This similarity suggests that any difference between the ratio of polar to apolar groups buried for protein and for RNA should have only a minimal effect on their overall interaction with urea, and a similar *m* value should be expected.

Empirically, the linear approximation of Δ*G* with urea concentration is accurate over an extended range of urea concentrations for both protein and RNA. Similarly, the transfer free energy of the side chains and polypeptide backbone for transfer from water to a solution of denaturant is observed to be linearly proportional to denaturant concentration (*41*, *42*). The observed linearity for protein and

RNA suggests that if a binding model is applicable, the binding is weak and the stability can be approximated using $\ln(1 + x) \sim x$ when $x \ll 1$, as

$$\Delta G(\text{urea}) = \Delta G(0) - \Delta nRT \ln(1 + K_b[\text{urea}]) \sim \Delta G(0) - \Delta nRTK_b[\text{urea}] \quad (8)$$

where Δn is the difference in the number of denaturant binding sites and K_b is the binding constant for each site.

CONCLUSIONS

An isothermal urea titration can be used reliably to measure the folding free energy of secondary and tertiary RNA structures. The linear extrapolation method, while assuming no physical mechanism for the action of urea, provides a thermodynamic parameter, the *m* value. Empirically, this parameter correlates linearly with the change in surface area in RNA folding. Hence, the *m* value provides a useful measure of the magnitude of the structural change in an RNA folding transition.

ACKNOWLEDGMENT

We thank Drs. Xing-wang Fang and Kim Sharp for enlightening discussions. We also thank the referees for their useful comments.

REFERENCES

1. Pace, C. N. (1975) *CRC Crit. Rev. Biochem. 3*, 1−43.
2. Myers, J. K., Pace, C. N., and Scholtz, J. M. (1995) *Protein Sci. 4*, 2138−2148.
3. Pan, T., and Sosnick, T. R. (1997) *Nat. Struct. Biol. 4*, 931−938.
4. Sclavi, B., Woodson, S., Sullivan, M., Chance, M. R., and Brenowitz, M. (1997) *J. Mol. Biol. 266*, 144−159.
5. Pan, J., Thirumalai, D., and Woodson, S. A. (1997) *J. Mol. Biol. 273*, 7−13.
6. Treiber, D. K., Rook, M. S., Zarrinkar, P. P., and Williamson, J. R. (1998) *Science 279*, 1943−1946.
7. Rook, M. S., Treiber, D. K., and Williamson, J. R. (1998) *J. Mol. Biol. 281*, 609−620.
8. Freier, S. M., Kierzek, R., Jaeger, J. A., Sugimoto, N., Caruthers, M. H., Neilson, T., and Turner, D. H. (1986) *Proc. Natl. Acad. Sci. U.S.A. 83*, 9373−9377.
9. Milligan, J. F., and Uhlenbeck, O. C. (1989) *Methods Enzymol. 180*, 51−62.
10. Behlen, L. S., Sampson, J. R., and Uhlenbeck, O. C. (1992) *Nucleic Acids Res. 20*, 4055−4059.
11. Latham, J. A., and Cech, T. R. (1989) *Science 245*, 276−282.
12. Ehresmann, C., Baudin, F., Mougel, M., Romby, P., Ebel, J. P., and Ehresmann, B. (1987) *Nucleic Acids Res. 15*, 9109−9128.
13. Alden, C. J., and Kim, S. H. (1979) *J. Mol. Biol. 132*, 411−434.
14. van Holde, K., Johnson, W. C., and Ho, P. S. (1998) *Principles of Physical Biochemistry*, Prentice-Hall, Inc., Englewood Cliffs, NJ.
15. Cantor, C., and Schimmel, P. (1980) *Biophysical Chemistry: Part II*, W. H. Freeman and Co., New York.
16. Gray, D. M., Hung, S. H., and Johnson, K. H. (1995) *Methods Enzymol. 246*, 19−34.
17. Quigley, G. J., and Rich, A. (1976) *Science 194*, 796−806.
18. Kim, S.-H. (1979) in *Cold Spring Harbor Monograph Series 9A-9B* (Schimmel, P. R., Söll, D., and Abelson, J., Eds.) p 2, Cold Spring Harbor Laboratory Press, Cold Spring Harbor, NY.
19. Cole, P. E., Yang, S. K., and Crothers, D. M. (1972) *Biochemistry 11*, 4358−4368.
20. Crothers, D. M., Cole, P. E., Hilbers, C. W., and Shulman, R. G. (1974) *J. Mol. Biol. 87*, 63−88.
21. Lynch, D. C., and Schimmel, P. R. (1974) *Biochemistry 13*, 1841−1852.
22. Privalov, P. L., and Filimonov, V. V. (1978) *J. Mol. Biol. 122*, 447−464.
23. Sampson, J. R., and Uhlenbeck, O. C. (1988) *Proc. Natl. Acad. Sci. U.S.A. 85*, 1033−1037.
24. Hall, K. B., Sampson, J. R., Uhlenbeck, O. C., and Redfield, A. G. (1989) *Biochemistry 28*, 5794−5801.
25. Sampson, J. R., DiRenzo, A. B., Behlen, L. S., and Uhlenbeck, O. C. (1990) *Biochemistry 29*, 2523−2532.
26. Behlen, L. S., Sampson, J. R., DiRenzo, A. B., and Uhlenbeck, O. C. (1990) *Biochemistry 29*, 2515−2523.
27. Friederich, M. W., and Hagerman, P. J. (1997) *Biochemistry 36*, 6090−6099.
28. Maglott, E. J., Deo, S. S., Przykorska, A., and Glick, G. D. (1998) *Biochemistry 37*, 16349−16359.
29. Celander, D. W., and Cech, T. R. (1990) *Biochemistry 29*, 1355−1361.
30. Celander, D. W., and Cech, T. R. (1991) *Science 251*, 401−407.
31. Hertzberg, R. P., and Dervan, P. B. (1984) *Biochemistry 23*, 3934−3945.
32. Tullius, T. D., and Dombroski, B. A. (1986) *Proc. Natl. Acad. Sci. U.S.A. 83*, 5469−5473.
33. Shortle, D., Chan, H. S., and Dill, K. A. (1992) *Protein Sci. 1*, 201−215.
34. Smith, L. J., Fiebig, K. M., Scwhalbe, H., and Dobson, C. M. (1996) *Folding Des. 1*, R95−R107.
35. Holbrook, J. A., Capp, M. W., Saecker, R. M., and Record, M. T., Jr. (1999) *Biochemistry 38*, 8409−8422.
36. Zou, Q., Habermann-Rottinghaus, S. M., and Murphy, K. P. (1998) *Proteins 31*, 107−115.
37. Qu, Y., Bolen, C. L., and Bolen, D. W. (1998) *Proc. Natl. Acad. Sci. U.S.A. 95*, 9268−9273.
38. Zhou, H. X., Hull, L. A., Kallenbach, N. R., Mayne, L., Bai, Y., and Englander, S. W. (1994) *J. Am. Chem. Soc. 116*, 6482−6483.
39. Breslow, R., and Guo, T. (1990) *Proc. Natl. Acad. Sci. U.S.A. 87*, 167−169.
40. Chothia, C. (1975) *Nature 254*, 304−308.
41. Tanford, C. (1968) *Adv. Protein Chem. 23*, 121−282.
42. Tanford, C. (1970) *Adv. Protein Chem. 24*, 1−95.
43. Fang, X., Pan, T., and Sosnick, T. R. (1999) *Biochemistry 38*, 16840−16846.

BI991699S